

Enalapril inhibits inflammatory osteolysis induced by wear debris in a mouse model

Journal of International Medical Research

48(6) 1–9

© The Author(s) 2020

Article reuse guidelines:

sagepub.com/journals-permissions

DOI: 10.1177/0300060520931612

journals.sagepub.com/home/imr



Huanzhi Ma, Qin Zhang, Jun Shi, Yutong Gao,
Chengliang Sun and Wei Zhang 

Abstract

Objective: Aseptic loosening, the most frequent complication after total joint replacement, is probably caused by an inflammatory response to the shedding of wear debris from the implant. The only effective treatment is surgical revision. Using a mouse model, we investigated whether enalapril inhibits wear debris-induced inflammatory osteolysis.

Methods: Titanium (Ti) alloy particles were introduced, and calvarial bone from syngeneic mice was implanted into air pouches established in BALB/c mice. Histological and molecular analyses were performed with inflammatory tissue samples obtained from mice treated with and without enalapril.

Results: Enalapril inhibited tissue inflammation and inflammatory osteolysis induced by Ti particles, reducing pouch membrane thickness and decreasing inflammatory cell infiltration. In addition, enalapril inhibited the expression of the inflammatory cytokines vascular endothelial growth factor and tumor necrosis factor- α .

Conclusions: Our study provides evidence that enalapril inhibits Ti particle-induced inflammatory osteolysis, and it may be a potentially useful treatment for aseptic loosening.

Keywords

Enalapril, wear debris, vascular endothelial growth factor, osteolysis, tumor necrosis factor- α , inflammation, total hip replacement, aseptic loosening

Date received: 5 February 2020; accepted: 13 May 2020

Department of Orthopedics, Shandong Provincial Hospital Affiliated to Shandong First Medical University, Jinan, China

Corresponding author:

Wei Zhang, Department of Orthopedics, Shandong Provincial Hospital Affiliated to Shandong First Medical University, 9677 Jingshi Road, Jinan, Shandong 250001, China.

Email: weizhang80s@126.com

Introduction

Aseptic loosening (AL) is the most frequent complication after total joint replacement



Creative Commons Non Commercial CC BY-NC: This article is distributed under the terms of the Creative Commons Attribution-NonCommercial 4.0 License (<https://creativecommons.org/licenses/by-nc/4.0/>) which permits non-commercial use, reproduction and distribution of the work without further permission provided the original work is attributed as specified on the SAGE and Open Access pages (<https://us.sagepub.com/en-us/nam/open-access-at-sage>).

surgery, postoperatively affecting approximately 20% of patients. There are no effective approaches for preventing and treating this complication. In addition, its pathogenesis is only partially understood, with most investigators believing an inflammatory reaction is the principal cause of the osteolysis that ultimately leads to AL.^{1,2} During its clinical course, the inflammatory cytokines vascular endothelial growth factor (VEGF) and tumor necrosis factor (TNF)- α play critical roles in osteoclast proliferation. VEGF can exacerbate inflammation and boost osteoclast survival, thereby worsening inflammatory osteolysis,³ whereas TNF- α can trigger aseptic inflammation and the differentiation of osteoclast precursors into mature osteoclasts.⁴

Enalapril, as an orally active inhibitor of angiotensin-converting enzyme, can safely and effectively manage hypertension and heart failure in the clinic.⁵ In addition, several studies indicated that enalapril has anti-inflammatory activities.^{6,7} The underlying mechanism may involve its anti-angiogenic characteristics and ability to suppress pro-inflammatory cytokine production.^{8,9} Despite the anti-inflammatory properties of enalapril, it is unclear whether the drug can protect against wear debris-induced osteolysis. We therefore asked whether enalapril could (1) block titanium (Ti) alloy particle-induced inflammatory osteolysis and (2) inhibit VEGF and TNF- α production in our murine model.

Materials and methods

Ti alloy particles with a diameter of 0.1 to 20 μm were purchased from Alfa Aesar (Ward Hill, MA, USA). The average diameter of the particles was 2.9 μm according to the manufacturer's certificate of analysis. Ninety percent of the particles were <10 μm in diameter. After 72 hours of sterilization in 70% ethanol, the particles were given three washes in sterile

phosphate-buffered saline (PBS). They were then suspended in sterile PBS to a concentration of 15 mg/ml and maintained at 4°C until use.¹⁰ A *Limulus* assay (QCL-1000, Lonza, Basel Switzerland) was used to confirm that the solution was endotoxin-free at a threshold of <0.05 EU/mL.

Mouse model of osteolysis

All animal procedures were approved by the institutional animal care and use committee of Shandong Provincial Hospital Affiliated to Shandong University. Ten-week-old female BALB/c mice (N=24) were obtained from Shandong University Animal Center and randomly assigned to three experimental groups (eight mice/group). In each mouse, the dorsal area (2 \times 2 cm^2 in size) was washed and shaved, and an air pouch was established through the subcutaneous injection of 2 mL of sterile air. To maintain the pouch, 0.5 mL of sterile air was introduced each day. After 6 days, mice with established air pouches were intraperitoneally injected with pentobarbital as an anesthetic (50 mg/kg). Then, a 0.5-cm incision was made into the pouch, and a piece of calvarial bone (approximately 0.8 \times 0.6 cm^2 in size) from a genetically identical donor mouse was inserted. In addition, 0.3 mL of the particle suspension was introduced into the pouch to trigger an inflammatory response. Some pouches were injected with sterile PBS as a control. To close the pouch layers and skin incision, 4-0 Prolene sutures (Ethicon, Johnson & Johnson, New Brunswick, NJ, USA) were used. For some mice, enalapril (Baoji Guokang Bio-Technology, Baoji, China), dissolved in 0.9% saline, was intraperitoneally injected (25 mg/kg/day) 2 days before the introduction of the Ti particles and every day until the mice were killed. Ten days after the bone implantation, the mice were sacrificed in a carbon dioxide

chamber. The pouch membranes containing the implanted bone were explanted for histological and molecular analyses.

Histological and image analyses

All tissue specimens were fixed for 24 hours in 4% polyoxymethylene (pH = 7.4). After decalcification, the samples were processed and paraffin embedded. To assess pouch membrane inflammation and implant bone erosion, 6-mm-thick tissue sections were stained with hematoxylin and eosin and examined under a light microscopy (Olympus DP70, Olympus, Tokyo, Japan). Digital photomicrographs were obtained and analyzed using Image-Pro Plus software (Media Cybernetics, Roper Technologies, Sarasota, FL, USA). To evaluate the level of particle-induced inflammation in the air pouch, we measured both the pouch membrane thickness and the total number of infiltrated cells. To evaluate bone resorption, the ratio of the remaining area of the bone (RRAB, %) and eroded surface area (ESA, mm²) were determined in the round region of interest, as described previously.^{11,12} For each specimen, pouch membrane thickness was determined at six different points in four different sections. The total numbers of infiltrated cells (cells/mm²) were determined by counting nuclei in six random 100- μ m-long pouch areas.¹³

Gene expression of VEGF and TNF- α

Total RNA was extracted from each pouch using TRIzol (Invitrogen, Thermo Fisher Scientific, Waltham, MA, USA) and used to synthesize cDNA. Quantitative real-time RT-PCR (qPCR) analysis was performed using SYBR Green (RR420, TaKaRa, Kyoto, Japan) in an ABI7500 system (Applied Biosystems, Thermo Fisher Scientific) to determine the relative expression levels of VEGF and TNF- α .

Primers against VEGF and TNF- α were designed using Primer 5.0. To standardize the target gene level as a result of varying RNA and cDNA quality, β -actin was co-amplified as an internal control. The qPCR primers were as follows: VEGF, forward, 5'-AAGATGCCGG TTCCAACCA-3', and reverse, 5'-CTTCTTCCAC CAC CGTGTCT-3'; TNF- α , forward, 5'-GAG TCCGGGC AGGTCTACTTT-3', and reverse, 5'-CAGGTCCTG TCCCAGC ATC T-3'; and β -actin, forward, 5'-CCTCTATGCC AACACAGTGC-3', and reverse, 5'-GTACTCCTGC TTGCTGAT CC-3'.

Immunohistological staining for TNF- α and VEGF

Paraffin-embedded sections were deparaffinized, washed briefly, heated for 15 minutes in antigen-retrieval buffer in a 98°C water bath, and then cooled to room temperature. They were next blocked for 1 hour in serum and incubated overnight at 4°C with goat anti-mouse VEGF antibody (15 μ g/mL; R&D Systems, Minneapolis, MN, USA) and rabbit anti-mouse TNF- α antibody (25 μ g/mL; Abcam). After washes, the sections were incubated for 1 hour at 37°C with biotin-conjugated secondary antibody, followed by the avidin-biotin-peroxidase complex. The colorimetric signal was developed through the addition of 3,3'-diaminobenzidine tetrahydrochloride. Using a \times 40 microscope objective, images of six random and representative fields from each section were obtained and analyzed with Image-Pro Plus software (Media Cybernetics).

Western blotting analysis

The protein concentrations of samples were determined using a quantitative protein analysis kit (Biocolor Bioscience & Technology Co., Shanghai, China). Equal amounts of protein (60 μ g) were separated

via 12% SDS-PAGE and transferred to a nitrocellulose membrane. After being blocked for 1 hour at room temperature in 5% non-fat milk containing 0.5% Tween-20, the membranes were incubated overnight at 4°C with rabbit anti-mouse TNF- α antibody (5 μ g/ml, Abcam, Cambridge, UK) or goat anti-mouse VEGF antibody (0.1 μ g/ml, R&D Systems) as the primary antibody. β -actin antibody (Abcam) was used as a loading control. After washes in Tris-buffered saline containing Tween-20 (TBST), the membranes were incubated at room temperature for 1 hour with the appropriate secondary antibody and then washed three times in TBST. Protein bands were visualized using the chemiluminescent method, and measured using a LAS-4000 Mini imager (FUJIFILM, Tokyo, Japan).

Statistical analysis

All statistical comparisons were performed using analysis of variance in SPSS version 20.0 (IBM, Armonk, NY, USA). Data are presented as the mean \pm standard deviation. Differences were considered statistically significant at $p < 0.05$.

Ethics and consent

All animal procedures were approved by the Institutional Animal Care and Use Committee of Shandong Provincial Hospital Affiliated to Shandong University (Jinan, China) and were performed in accordance with the guidelines for the ethical care of animals (approval no. 2018-017).

Results

Enalapril inhibits Ti particle-induced inflammatory osteolysis and tissue inflammation

Our data illustrated that enalapril inhibited Ti alloy particle-induced tissue inflammation. Pouches injected with Ti particles displayed inflammatory changes versus the findings in control saline-injected pouches (Figure 1a and 1b). However, enalapril significantly relieved inflammation within the pouch (Figure 1c). The membrane thickness of the air pouches and the total numbers of cells were calculated to assess particle-induced inflammation.¹⁴ The membrane thickness in the air pouches exposed to Ti particles ($198 \pm 35.2 \mu\text{m}$, Figure 2a) was significantly higher than that of saline-injected controls ($133 \pm 32.6 \mu\text{m}$, $P < 0.05$).

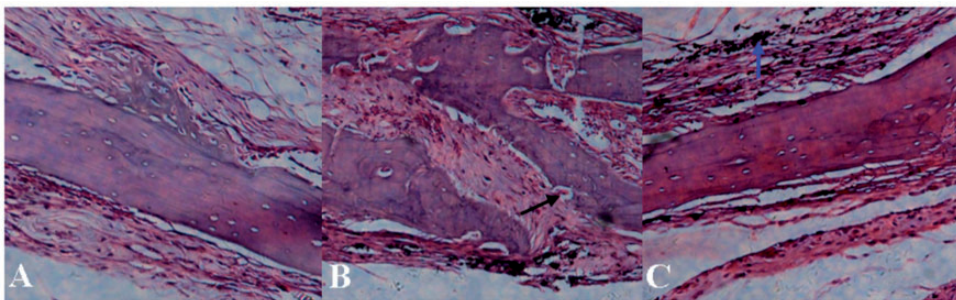


Figure 1. Typical histological appearance of calvarial bone-implanted pouch tissues.

(a) Control pouch, (b) titanium (Ti)-implanted pouch, and (c) Ti-implanted pouch treated with enalapril. Tissue sections were stained with hematoxylin and eosin and imaged at $\times 200$ magnification. Ti particles are marked by blue arrows. Erosion is visible of the implanted calvarial bone in (b) (black arrow). (c) Enalapril treatment markedly ameliorated the erosion.

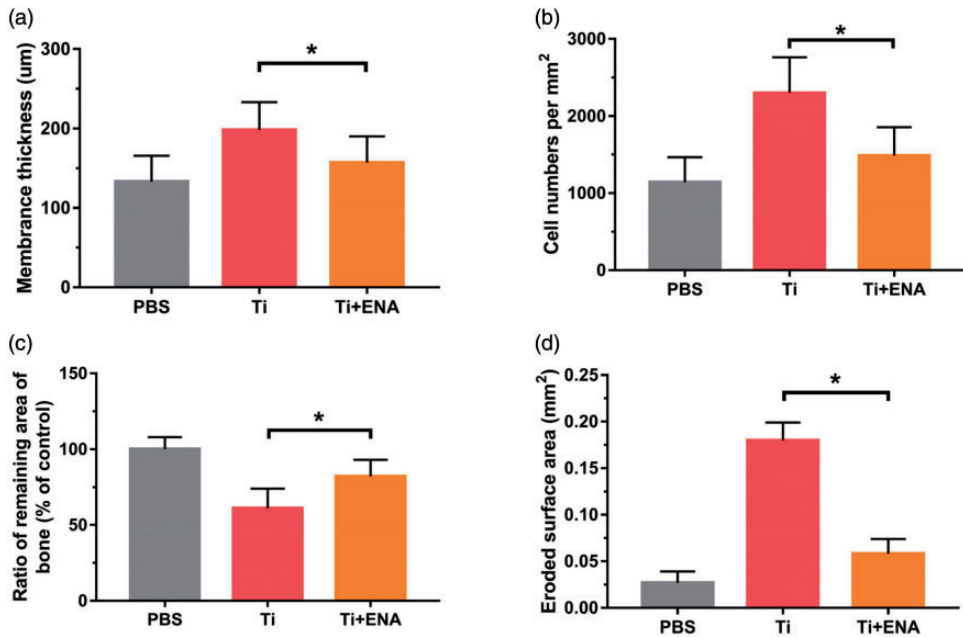


Figure 2. Enalapril prevented titanium (Ti) particle-induced inflammatory osteolysis. Histological analysis of membrane thickness (a), total cell counts (b), the ratio of remaining area of bone (c), and the eroded surface area (d) in Ti-exposed pouches. Four sections per specimen were assessed in a blinded manner using Image-Pro Plus software. Data are expressed as the mean \pm standard deviation (8 mice/group). * $P < 0.05$.

Cell infiltration was also significantly higher in Ti-stimulated pouches (cell number, 2298 ± 464) than in control pouches (cell number, 1142 ± 324 , $P < 0.05$, Figure 2b). Importantly, enalapril treatment significantly decreased Ti particle-induced membrane thickness ($157 \pm 33.1 \mu\text{m}$, $P < 0.05$) and cell infiltration (cell number, 1485 ± 372 , $P < 0.05$). Bone resorption was significantly lower in enalapril-treated mice than in control mice as measured using RRAB and ESA (both $P < 0.05$; Figure 2c and 2d).

Enalapril inhibits TNF- α and VEGF expression

We examined the mRNA levels of VEGF and TNF- α in the mouse model using qPCR (Figure 3). Our data revealed that

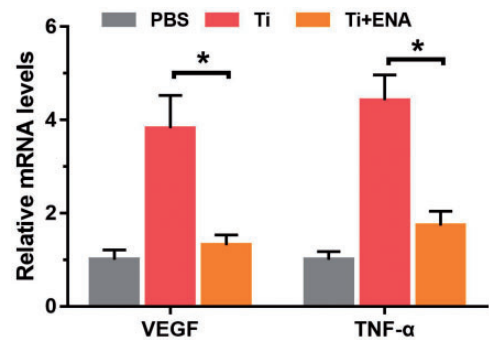


Figure 3. Effects of enalapril on the gene expression of vascular endothelial growth factor (VEGF) and tumor necrosis factor (TNF)- α in pouch tissues. Compared with the control, VEGF (3.8-fold) and TNF- α (4.4-fold) gene expression was markedly increased in pouch tissues exposed to Ti particles. This increase was significantly blocked by enalapril (analysis of variance). * $P < 0.05$.

their levels were significantly upregulated in the Ti particle-stimulated group versus the PBS control group ($P < 0.05$), and enalapril treatment significantly blocked this increase ($P < 0.05$).

Next, the protein levels of VEGF and TNF- α in air pouch membranes were evaluated using immunohistochemical staining. As shown in Figure 4a, higher staining of both VEGF and TNF- α was found in Ti-containing pouches versus the findings for the control. However, in enalapril-treated tissues, VEGF and TNF- α levels were significantly reduced as indicated by the percentages of cells with positive

VEGF and TNF- α staining (both $P < 0.05$, Figure 4b).

The protein levels of VEGF and TNF- α were also measured using western blotting. Higher densitometric values were found for both VEGF (Figure 5a) and TNF- α (Figure 5b) in Ti-containing pouches than in control pouches, and their levels were reduced by enalapril treatment (both $P < 0.05$).

Discussion

Total joint replacement is a generally successful procedure that is widely used clinically to restore joint function, reduce pain,

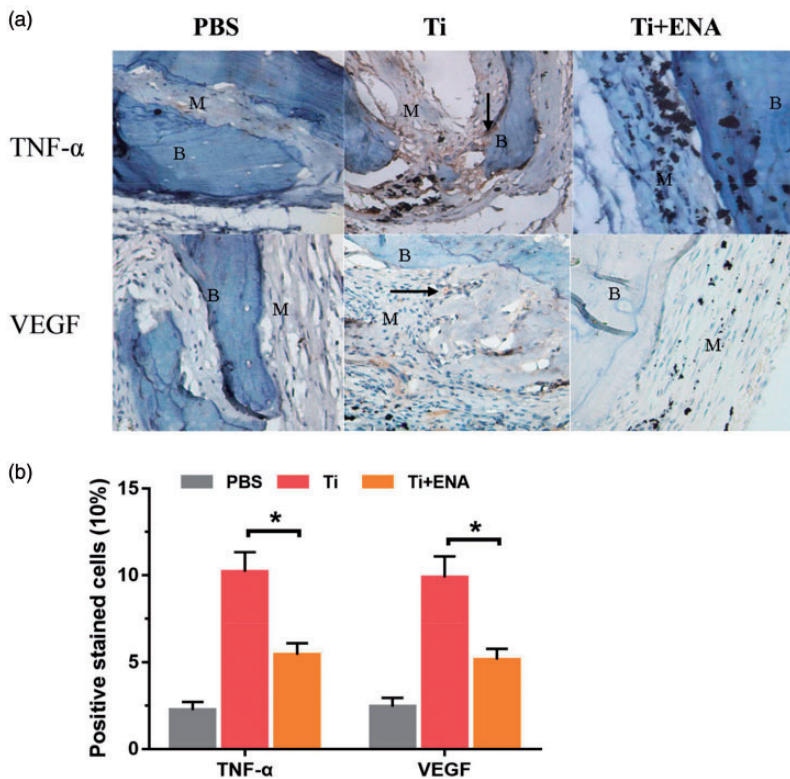


Figure 4. Immunohistochemical staining of tumor necrosis factor (TNF)- α and vascular endothelial growth factor (VEGF). (a) Immunohistochemical staining of TNF- α and VEGF (original magnification, $\times 200$). Positive staining is indicated by arrowheads. B, Bone implant; M, air pouch membrane. (b) Positively stained cells were identified using Image-Pro Plus software as described in the Materials and Methods. The number indicates the percentage of positively stained cells. * $P < 0.05$.

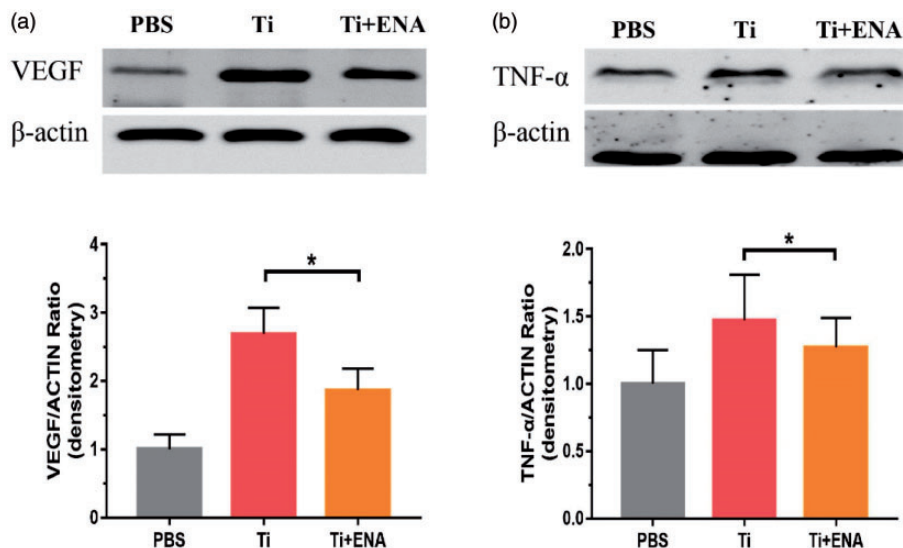


Figure 5. Western blot of vascular endothelial growth factor (VEGF) and tumor necrosis factor (TNF)- α . The protein levels of VEGF (a) and TNF- α (b) were examined. β -actin served as a loading control. Densitometric results from three separate western blotting experiments. * $P < 0.05$.

and allow patients with arthritis to resume various activities of daily living. However, a considerable number of patients experience AL after joint replacement. The only effective corrective approach for AL is surgical revision. One newer strategy involves the development of a novel pharmacological approach to ameliorate AL-related inflammatory osteolysis. Because enalapril has anti-inflammatory activity, we wondered whether the drug can inhibit the development of AL.

To reflect the clinical situation, we developed a mouse model featuring an air pouch implanted with cranial bone. Our results revealed that enalapril injection could relieve inflammatory osteolysis in Ti-exposed tissue. The infusion of Ti alloy particles triggered inflammatory osteolysis in the region of the pouch. Enalapril decreased the pouch membrane thickness, bone resorption, and inflammatory cell infiltration, illustrating that the drug can reduce Ti-associated tissue inflammation and inflammatory osteolysis.

Enalapril likely acts by inhibiting pro-inflammatory cytokine production and osteoclast differentiation., VEGF and TNF- α expression was upregulated in mice with Ti alloy particle-induced inflammatory osteolysis. However, enalapril blocked this increase. VEGF, a major pro-angiogenic cytokine released by fibroblasts, macrophages, endothelial cells, and other cell types,¹⁵ is a key player in the initiation and durability of inflammation, and it promotes osteoarthritis and rheumatoid arthritis.¹⁶ VEGF is currently considered a central regulator of osteoclastogenesis (i.e., bone resorption), and inflammatory osteoclastogenesis is a vital step in the establishment of AL.^{17,18} VEGF directly targets osteoclasts, boosting their survival.¹⁹ In addition, VEGF participates in the process of wear debris-induced inflammatory osteolysis and vascularizes granulomatous periprosthetic tissue, which could promote the progression of AL. Our study confirmed that VEGF was upregulated during inflammatory osteolysis. However, enalapril

injection reduced the increase in VEGF expression. These results provide evidence that enalapril has a strong inhibitory effect on VEGF production.

Produced by macrophages, the pro-inflammatory cytokine TNF- α plays vital roles in the response to particles and the development of AL.²⁰ AL is partly caused by wear debris-induced inflammation of the membrane around the prosthesis. Periprosthetic tissue inflammation occurs simultaneously with the local accumulation of pro-inflammatory cytokines such as TNF- α , interleukin (IL)-1 β , and IL-6. Of these, TNF- α is the principal pro-inflammatory cytokine, and it controls the release of other pro-inflammatory mediators such as IL-6 and IL-1 β .²¹ In addition, TNF- α is critically involved in bone resorption and osteoclastogenesis during periprosthetic osteolysis. Both the RNA and protein levels of TNF- α were increased by Ti particle-induced inflammatory osteolysis. Similarly as VEGF, TNF- α was markedly downregulated in mice treated with enalapril. Given the predominant effect of TNF- α on periprosthetic tissue, the inhibitory effect of enalapril on TNF- α might be one strategy to reduce the wear debris-related chronic inflammation common to periprosthetic tissue.

Our findings suggest that enalapril is a promising therapy for preventing and treating AL. Enalapril could possibly be used as a preventive measure when joint replacement is performed or as a treatment when serial X-rays demonstrate early signs of osteolysis and loosening after joint replacement. Nevertheless, further work is required to examine and verify the potential clinical applications of enalapril for AL.

Conclusion

Our results revealed that enalapril can inhibit inflammatory osteolysis in a mouse model of osteolysis. Our evidence

illustrating the strong inhibitory effect of enalapril on inflammatory osteolysis has potential clinical importance.


Declaration of conflicting interest

The authors declare that there is no conflict of interest.

Funding

This work was supported by grants from the National Natural Science Foundation of China (No. 81201441).

ORCID iD

Wei Zhang  <https://orcid.org/0000-0002-0747-8184>

References

- Holt G, Murnaghan C, Reilly J, et al. The biology of aseptic osteolysis. *Clin Orthop Relat Res* 2007; 460: 240–252.
- Zhang K, Yang SY, Yang S, et al. Different influence of Ti, PMMA, UHMWPE, and Co-Cr particles on peripheral blood monocytes during periprosthetic inflammation. *J Biomed Mater Res A* 2015; 103: 358–364.
- Yang Q, McHugh KP, Patntirapong S, et al. VEGF enhancement of osteoclast survival and bone resorption involves VEGF receptor-2 signaling and beta3-integrin. *Matrix Biol* 2008; 27: 589–599.
- Kitaura H, Zhou P, Kim HJ, et al. M-CSF mediates TNF-induced inflammatory osteolysis. *J Clin Invest* 2005; 115: 3418–3427.
- Ku LC, Zimmerman K, Benjamin DK, et al. Safety of Enalapril in Infants Admitted to the Neonatal Intensive Care Unit. *Pediatr Cardiol* 2017; 38: 155–161.
- Ding LH, Liu D, Xu M, et al. Enalapril inhibits tubulointerstitial inflammation and NLRP3 inflammasome expression in BSA-overload nephropathy of rats. *Acta Pharmacol Sin* 2014; 35: 1293–1301.
- Penitente AR, Leite AL, De Paula Costa G, et al. Enalapril in Combination with Benznidazole Reduces Cardiac Inflammation and Creatine Kinases in Mice Chronically

- Infected with *Trypanosoma cruzi*. *Am J Trop Med Hyg* 2015; 93: 976–982.
8. Ghosh SS, Krieg R, Massey HD, et al. Curcumin and enalapril ameliorate renal failure by antagonizing inflammation in 5/6 nephrectomized rats: role of phospholipase and cyclooxygenase. *Am J Physiol Renal Physiol* 2012; 302: F439–F454.
 9. Rani N, Bharti S, Tomar A, et al. Inhibition of PARP activation by enalapril is crucial for its renoprotective effect in cisplatin-induced nephrotoxicity in rats. *Free Radic Res* 2016; 50: 1226–1236.
 10. Zhang W, Peng X, Cheng T, et al. Vascular endothelial growth factor gene silencing suppresses wear debris-induced inflammation. *Int Orthop* 2011; 35: 1883–1888.
 11. Li Y, Li J, Li B, et al. Anthocyanin suppresses CoCrMo particle-induced osteolysis by inhibiting IKK α/β mediated NF- κ B signaling in a mouse calvarial model. *Mol Immunol* 2017; 85: 27–34.
 12. Kauther MD, Neuerburg C, Wefelnberg F, et al. RANKL-associated suppression of particle-induced osteolysis in an aged model of Calcitonin and α -CGRP deficiency. *Biomaterials* 2013; 34: 2911–2919.
 13. Peng X, Tao K, Cheng T, et al. Efficient Inhibition of wear debris-induced inflammation by locally delivered siRNA. *Biochem Biophys Res Commun* 2008; 377: 532–537.
 14. Sud S, Yang SY, Evans CH, et al. Effects of cytokine gene therapy on particulate-induced inflammation in the murine air pouch. *Inflammation* 2001; 25: 361–372.
 15. Ferrara N, Gerber HP and LeCouter J. The biology of VEGF and its receptors. *Nat Med* 2003; 9: 669–676.
 16. Greenfield EM, Bi Y, Ragab AA, et al. The role of osteoclast differentiation in aseptic loosening. *J Orthop Res* 2002; 20: 1–8.
 17. Cheng T, Zhao Y, Li B, et al. Curcumin Attenuation of Wear Particle-Induced Osteolysis via RANKL Signaling Pathway Suppression in Mouse Calvarial Model. *Mediators Inflamm* 2017; 2017: 5784374.
 18. Wooley PH and Schwarz EM. Aseptic loosening. *Gene Ther* 2004; 11: 402–407.
 19. Ren WP, Markel DC, Zhang R, et al. Association between UHMWPE particle-induced inflammatory osteoclastogenesis and expression of RANKL, VEGF, and Flt-1 in vivo. *Biomaterials* 2006; 27: 5161–5169.
 20. Zhang W, Zhao H, Peng X, et al. Low-dose captopril inhibits wear debris-induced inflammatory osteolysis. *J Int Med Res* 2011; 39: 798–804.
 21. Xiang B, Zhong P, Fang L, et al. miR-183 inhibits microglia activation and expression of inflammatory factors in rats with cerebral ischemia reperfusion via NF- κ B signaling pathway. *Exp Ther Med* 2019; 18: 2540–2546.